Year 2 Final Report: Evaluation and Improvement of Ocean Model Parameterizations for NCEP Operations

PI: Dr. Lynn K. Shay
Co-PI: George Halliwell
NCEP Collaborator: Dr. Carlos Lozano

RSMAS/MPO, University of Miami – 4600 Rickenbacker Causeway, Miami, FL 33149, USA
Phone: (305) 421-4075 - Fax: (305) 421-4696 - Email: nick@rsmas.miami.edu –
Internet: http://isotherm.rsmas.miami.edu/~nick

Goal: The long term goal of this NOAA Joint Hurricane Testbed (JHT) grant is to evaluate and improve ocean model parameterizations in NOAA National Centers for Environmental Prediction (NCEP) coupled hurricane forecast models in collaboration with the NOAA Tropical Prediction Center (TPC) and NOAA/NCEP Environmental Modeling Center (EMC). This effort targets the Joint Hurricane Testbed programmatic priorities **EMC-1** and **EMC-2** along with hurricane forecaster priorities **TPC-1** and **TPC-2** that focus on improving intensity forecasts through evaluating and improving oceanic boundary layer performance in the coupled model and improving observations required for model initialization, evaluation, and analysis. This project will be conducted under the auspices of the Cooperative Institute of Marine and Atmospheric Science program, and addresses **CIMAS Theme 5: Air-Sea Interactions and Exchanges** and **NOAA Strategic Goal 3: Weather and Water (local forecasts and warnings)**.

Specific objectives of this grant are:

i) optimizing spatial resolution that will permit the ocean model to run efficiently as possible without degrading the simulated response;
ii) improving the initial background state provided to the ocean model;
iii) improving the representation of vertical and horizontal friction and mixing;
iv) generating the realistic high-resolution atmospheric forcing fields necessary to achieve the previous objectives; and
v) interacting with NOAA/NCEP/EMC in implementing ocean model code and evaluating the ocean model response in coupled hurricane forecast tests

Progress: This applied effort has proceeded along two closely related tracks: the preparation and analysis of the *in-situ* ocean observations required to evaluate ocean model performance, and the thorough evaluation of ocean model performance using these and other available ocean observations. The observational effort includes processing in situ Acoustic Doppler Current Profiler (ADCP) data from Ivan (provided by the U.S. Naval Research Laboratory), moored observations during Katrina and Rita (data courtesy of Minerals Management Service-MMS), and NOAA Hurricane Research Division (HRD) Intensity Fluctuation Experiments (IFEX) observations for pre and post Rita in 2005 (Rogers *et al.*, 2006; Jaimes and Shay, 2009). In addition, oceanic and atmospheric profiler measurements were acquired during hurricanes Gustav and Ike in 2008 in and over the Gulf of Mexico. In all these cases, satellite observations (altimetry and SST) have been obtained and Ocean Heat Content (OHC) maps have been produced.

The centerpiece of the modeling effort to date is a thorough evaluation of ocean model performance during Hurricane Ivan (2004) designed to address the specific objectives listed above. A paper describing these results (Halliwell *et al.*, 2010) submitted to *Monthly Weather Review* is now undergoing revision. Reference experiments have also been performed for Hurricanes Katrina and Rita. These experiments have demonstrated that accurate ocean model initialization with respect to upper-ocean temperature and salinity (density) profiles along with the correct location of ocean currents and eddies is the most important factor influencing the accuracy of SST cooling forecast by an ocean model. Efforts are now underway to evaluate existing ocean model initialization products prior to a large number of storms to quantify errors and biases and to design observational strategies to improve the initial ocean fields. During the second year of this project, G. Halliwell moved from RSMAS to NOAA/AOML and is now working with HRD modelers on the experimental HWRF coupled forecast model (HWRF-X) as part of the Hurricane Forecast Improvement Program (HFIP). As this JHT project transitions to the two-year continuation project, Halliwell will extend the ocean model evaluation effort to the impact of ocean model sensitivities on TC forecast errors, particularly for intensity. This will improve our capability to address the objectives listed above and recommend ocean model improvement strategies to NOAA/NCEP/EMC.

Modeling: The Hybrid Coordinate Ocean Model (HYCOM) is the chosen ocean model because it is being evaluated as the ocean model component of the next-generation coupled hurricane forecast model under development at NOAA/NCEP/EMC. It also contains multiple choices of numerical schemes and subgrid-scale parameterizations, making it possible to isolate model sensitivity to individual processes and devise strategies to improve model representation of these processes. In this context, fifteen free-running HYCOM simulations were conducted to assess model sensitivity to vertical resolution in the surface mixed layer, horizontal resolution, vertical mixing scheme, wind stress drag coefficient, surface turbulent flux drag coefficient, resolution of surface forcing, accuracy of ocean model initialization, and ocean dynamics (one dimensional versus three dimensional) for hurricane Ivan (numerical experiments are listed in Table 1). All experiments were conducted within a GOM domain where the coastline follows the actual land/sea boundary with a minimum water depth of 2 m. They are all nested within an outer model and are forced by surface fields of vector wind stress, wind speed, surface atmospheric temperature and humidity, longwave and shortwave radiation, and precipitation. Surface turbulent heat fluxes and evaporation are calculated during model runs using bulk formula. Freshwater input from 12 rivers is included. A control experiment (GOM1) is performed that is forced by atmospheric fields from the 27 km resolution COAMPS model, but with high-resolution wind speed and stress fields obtained from the NOAA/HRD HWIND analysis patched in for the storm region. HWIND vector wind fields are first patched into COAMPS wind fields, and then wind stress is calculated using bulk formula with the Donelan *et al.* (2003) drag coefficient prior to model runs. The model is nested within a GOM data-assimilative hindcast that uses the U. S. Navy NCODA system. It is run with 26 vertical layers and KPP vertical mixing is used. Surface turbulent fluxes are calculated during the model run using the COARE 2.6 algorithm bulk formula. Attributes of the control experiment are summarized in Table 1.

The remaining experiments all differ from GOM1 by altering one single model attribute (Table 1). GOM2 isolates sensitivity to horizontal resolution, GOM3 and GOM4 to vertical resolution, GOM5 and GOM6 to vertical mixing scheme, GOM7-GOM11 to wind stress drag coefficient parameterization, GOM12 to turbulent heat flux drag coefficient representation, GOM13 to surface forcing resolution (COAMPS without HWIND patching), GOM14 to ocean model initialization (nesting within a non-assimilative ocean model), and GOM15 to one-dimensional

ocean dynamics. Model sensitivities are initially evaluated by calculating the changes in SST that occurred between 11 and 17 September 2004 (before and after Ivan). RMS differences between temperature changes produced by the control experiment and each of the other 14 experiments (Figure 1) quantify the sensitivity to the individual model attribute that was altered from the control experiment. It is immediately evident in Figure 1 that accurate initialization of ocean features (GOM14) is the most important single factor for improving the accuracy of the ocean response. The second most important factor is ocean dynamics because the impact of wind-driven upwelling and pre-existing ocean currents exert a large impact on the magnitude and pattern of SST cooling. Four factors are of intermediate importance: (1) parameterization of surface momentum flux through the drag coefficient (GOM7-GOM11); (2) choice of vertical mixing scheme (GOM5, GOM6); (3) horizontal resolution (GOM2); and (4) adequate resolution of the storm structure by the surface forcing (GOM14). The least important factors are vertical resolution (GOM3, GOM4) and the parameterization of surface heat flux through the sensible and latent heat drag coefficients (GOM11). For vertical resolution, larger RMS differences are observed going from 21 to 26 layers than from 26 to 31 layers. Consistent with Jacob *et al.* results from a previous Vertical Mixing JHT grant, these diminishing returns with increasing resolution suggest that the intermediate vertical resolution (26 layers, 4-8 m resolution in the mixed layer) is a reasonable choice.

Table 1. Summary of the 15 numerical experiments simulating the ocean response to hurricane Ivan conducted in the GOM domain. Key model attributes that are varied are broken into major categories and listed in column 1. Characteristics of the control experiment are listed in column 2 while the single model attributes varied in each of the remaining experiments are listed in column 3.

Model Attribute	Control Experiment (**GOM1**)	Alternate Experiments
Horizontal resolution	0.04° Mercator	**GOM2**: 0.08° Mercator
Vertical resolution	26 layers, 4-8m in OML	**GOM3**: 21 layers, 7.5-15m in OML **GOM4**: 31 layers, 3-5m in OML
Vertical mixing	KPP	**GOM5**: MY **GOM6**: GISS
C_D	Donelan	**GOM7**: Powell **GOM8**: Large and Pond **GOM9**: Large and Pond (capped) **GOM10**: Shay and Jacob **GOM11:** Jarosz *et al.*
C_{EL}, C_{ES}	COARE3.0 algorithm	**GOM12**: Kara *et al.*
Atmospheric forcing	27-km COAMPS+H*WIND	**GOM13**: 27-km COAMPS only
Outer model	NCODA GOM hindcast	**GOM14**: Free GOM simulation
Ocean dynamics	Three-dimensional	**GOM15**: One-dimensional

SST Response Evaluation: Halliwell *et al.* (2010) evaluate the simulated SST cooling patterns forced by Ivan against daily SST fields generated by the objective analysis of *in-situ* observations along with AVHRR and microwave satellite observations onto a 0.25° global grid (Reynolds *et al.*, 2007), hereinafter referred to as "blended" SST. The mean differences listed in Table 2 demonstrate that in the subdomain over which these analyses were performed (delineated by the boxes within the four inset panels in Figure 1), the ocean model did not cool as much as

indicated by the blended SST fields. Although the model overcooled within a cold-core cyclone centered near 25°N, 87°W by >4°C (Halliwell *et al.*, 2010), this overcooling was more than compensated for by undercooling over the remainder of the domain. Mean differences display the largest sensitivity to ocean model initialization, surface forcing resolution, and wind stress drag coefficient, with more (less) cooling occurring for larger (smaller) values of C_D. Smaller sensitivity is evident for vertical mixing choice, with the MY and GISS schemes producing slightly more cooling than KPP. Little sensitivity is evident to vertical and horizontal resolution. RMS differences between the simulations and blended SST are substantially increased by the large simulated overcooling in the cold-core cyclone centered near 25°N, 87°W.

Table 2. Comparison of ΔT (^{o}C: temperature change forced by Ivan) images (17Sept. -10 Sept.) between the 15 experiments and blended SST data product: mean differences (column 2) within the subdomain outlined by the boxes in the inset maps of Figure 1 and RMS differences within the same domains (column 3).

Experiment	ΔT Mean Difference (°C)	ΔT RMS Difference (°C)
GOM1	0.24	1.33
GOM2	0.25	1.29
GOM3	0.30	1.40
GOM4	0.22	1.40
GOM5	0.30	1.26
GOM6	0.47	1.33
GOM7	0.38	1.33
GOM8	0.04	1.57
GOM9	0.14	1.47
GOM10	-0.19	1.71
GOM11	0.06	1.37
GOM12	0.11	1.34
GOM13	0.51	1.24
GOM14	0.84	1.51
GOM15	0.06	1.55

Halliwell *et al*. (2010) further evaluates the fidelity of simulated SST cooling patterns using advanced analysis techniques, specifically Taylor (2001) diagrams and the Murphy (1988) skill scores (not shown). Summarizing the overall conclusions, the control experiment produced one of the most realistic SST response patterns as expected. Three experiments stood out as much inferior to the control experiment, specifically GOM13 (low-resolution atmospheric forcing, GOM14 (alternate initialization) and GOM15 (one-dimensional ocean dynamics). All other experiments produced SST cooling patters that were equally correlated with cooling in the blended analysis (≈0.7), but some of the wind stress drag coefficient choices degraded the realism of the cooling response. Drag coefficient values substantially smaller than the Donelan choice used in the control experiment tended to underestimate the magnitude of the cooling pattern (GOM7) while values substantially larger than Donelan substantially overestimated the

magnitude of the cooling pattern (GOM8, GOM10). The quality of the eight other experiments was almost identical to the quality of the control experiment. However, this does not mean that all of the model attributes evaluated in these eight experiments will have an insignificant influence on storm intensity. For example, although the SST cooling pattern was only slightly different among the three vertical mixing choices (GOM1, GOM5, GOM6), they produced potentially significant differences in the turbulent heat flux from ocean to atmosphere (up to 200 W m^{-2}) beneath the inner core of the storm. Although changing the surface turbulent heat flux parameterization (GOM12) had little influence on the SST cooling pattern, it also had a potentially significant influence on the heat flux (differences up to 300 W m^{-2}). Further details on model evaluation are contained in Halliwell *et al.* (2010).

Alternate Experiment	Model Attribute Changed from Control Experiment	ΔT (C) Mean Diff.	ΔT (C) RMS
GOM2	Low horizontal resolution	+0.01	0.47
GOM3	Low vertical resolution	+0.05	0.29
GOM4	High vertical resolution	-0.02	0.26
GOM5	MY mixing	+0.06	0.49
GOM6	GISS mixing	+0.21	0.37
GOM7	Powell C_D	+0.13	0.33
GOM8	Large&Pond C_D	-0.19	0.48
GOM9	Large&Pond (capped) C_D	-0.08	0.19
GOM10	Shay&Jacob C_D	-0.39	0.75
GOM11	Jarosz *et al.* C_D	-0.04	0.28
GOM12	Kara *et al.* C_L, C_S	-0.13	0.18
GOM13	No H*WIND	+0.25	0.70
GOM14	Outer model	+0.43	1.57
GOM15	One-dimensional	-0.17	1.31

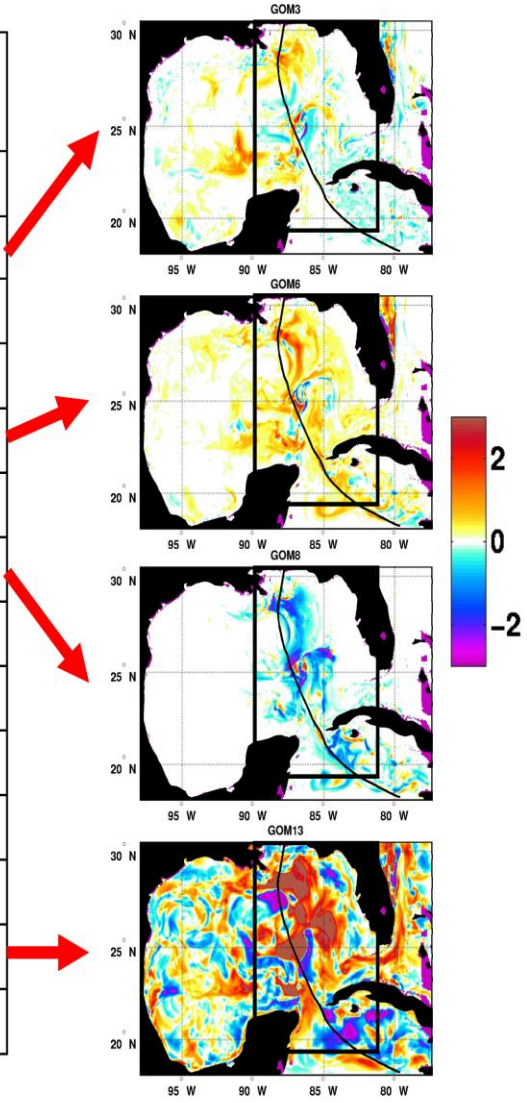

Figure 1. Sensitivity analysis of SST change (^oC) forced by hurricane Ivan, as summarized by differences in the SST change from Sept. 11 minus Sept. 17 produced by experiments GOM2-GOM15 and the control experiment GOM1. The mean cooling bias relative to the GOM1 and the RMS difference from the control experiment are tabulated and four images of the difference in SST cooling for the four experiments marked by red arrows are included for reference.

Measurements: Hurricane Ivan passed directly over 14 ADCP moorings that were deployed as part of the NRL *Slope to Shelf Energetics and Exchange Dynamics (SEED)* project from May through Nov 2004 (Teague *et al*. 2007) (Figure 2). These observations enable the simulated ocean current (and shear) response to a hurricane over a continental shelf/slope region to be evaluated. This evaluation also involves detailed comparisons between *in-situ* and satellite–derived OHC estimates based on Surface Height Anomaly (SHA) fields from available radar altimeters (NASA TOPEX, Jason-1, ERS-2, NOAA GEOSAT Follow-On-Missions), and infrared and microwave SSTs from TRMM and AMSR-E.

Table 3: Summary of measurements from four of the fourteen NRL SEED ADCP arrays (LR- Long Ranger, TRBM- Trawl Resistant Bottom Mount) spanning the coastal ocean (60 m) to the continental slope (1029 m). For the purposes of this brief report we will focus on Array 8 and 9 as they were located along Ivan's track (8) and at 1.5 R_{max} (9) to the right of the track.

Array #	Lat ^{o}N	Long ^{o}W	Start Date 2004	End Date 2004	Δt (hr)	Depth Range (m)	Δz (m)	Bottom Depth (m)	Instrument Type
2	29.43	88.01	05/01	10/31	**0.25**	4-54	**2**	**60**	TRBM
8	29.14	88.11	05/03	11/07	**1.0**	42-492	**10**	518	LR
9	29.19	87.94	05/03	11/07	**1.0**	40-500	**10**	518	LR
14	29.20	87.65	05/05	11/07	**1.0**	42-502	**10**	**1029**	LR

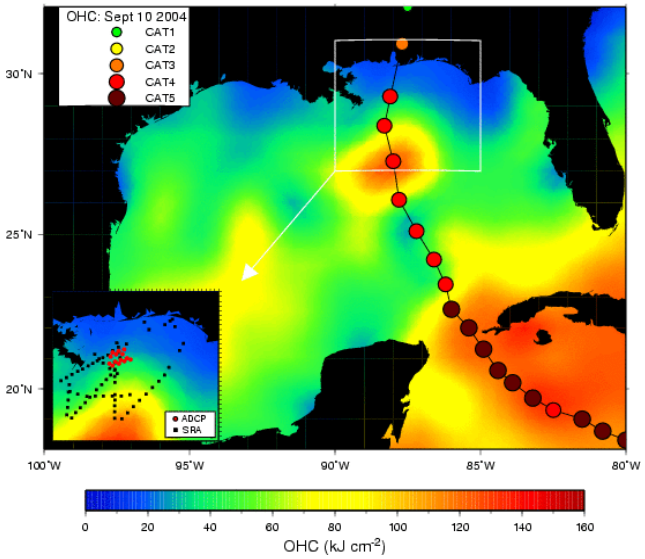

Figure 2: OHC map and inset showing NRL mooring locations (red) and SRA wave measurements (black) relative to Ivan's storm track and intensity. The OHC pattern shows the WCR encountered by Ivan prior to landfall. The cooler shelf water (OHC < 20 KJ cm-2) resulted from the passage of Frances two weeks earlier.

Current Profiler Analyses: As shown in Table 3, a synopsis of four of the fourteen ADCP arrays are summarized with respect to position, range of measurements temporal vertical sampling intervals as discussed by Teague *et al*. (2007). These profiler measurements provided the evolution of the current (and shear) structure from the deep ocean across the shelf break and over the continental shelf. The current shear response, estimated over 4-m vertical scales, is shown in Figure 3 based on objectively analyzed data from these moorings. Over the shelf, the

current shears increased due to hurricane Ivan strong winds. The normalized shear magnitude is a factor of four times larger over the shelf (depths of 100 m) compared to normalized values over the deeper part of the mooring array (500 to 1000 m). Notice that the current shear rotates anticyclonically (clockwise) in time over 6-h intervals consistent with the forced near-inertial response (periods slightly shorter than the local inertial period). In this measurement domain, the local inertial period is close to 24 h which is close to the diurnal tide. By removing the weaker tidal currents and filtering the records, the analysis revealed that the predominant response was due to forced near-inertial motions. These motions have a characteristic time scale for the phase of each mode to separate from the wind-forced OML current response when the wind stress scale ($2R_{max}$~64 km in Ivan during time of closest approach) exceeds the deformation radius associated with the first baroclinic mode (≈ 30 to 40 km). This time scale increases with the number of baroclinic modes due to decreasing phase speeds (Shay *et al.* 1998). The resultant vertical energy propagation from the OML response is associated with the predominance of the anticyclonic (clockwise) rotating energy with depth and time that is about four times larger than the cyclonic (counterclockwise) rotating component.

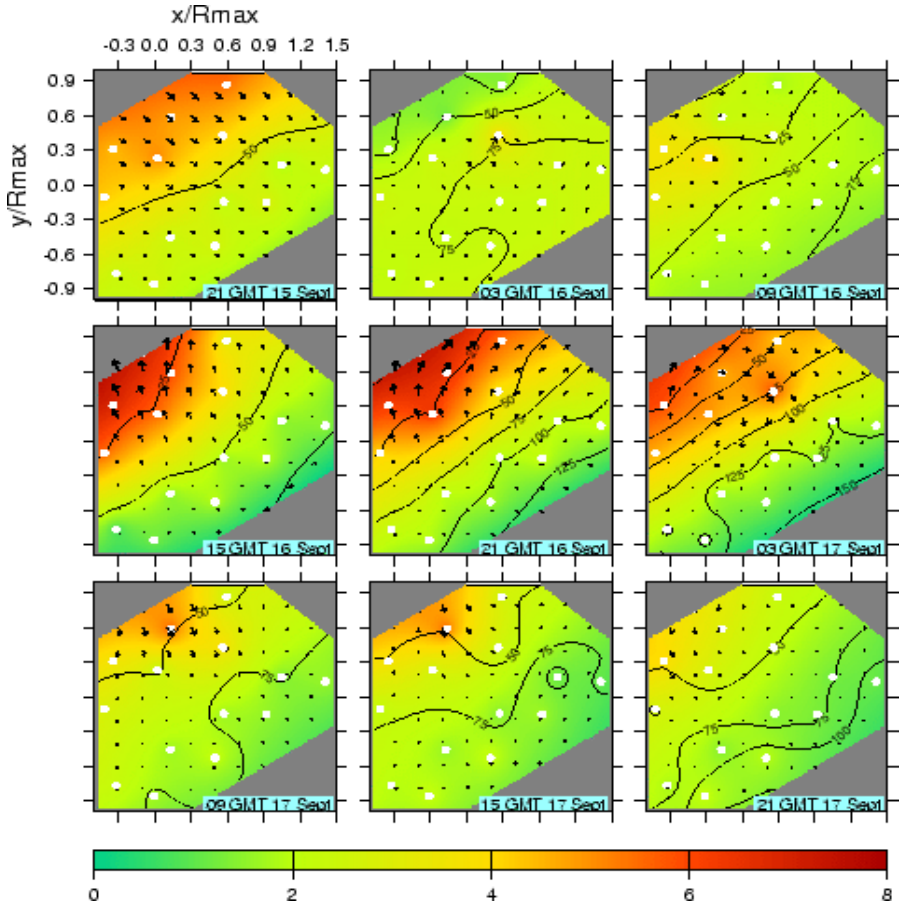

Figure 3: Spatial evolution of the rotated current shear magnitude normalized by observed shears from the ADCP measurements (white dots) normalized by observed shears in the Loop Current of 1.5 x 10^{-2} s^{-1} (color) during Lili starting at 2100 GMT 15 Sept every 6 hours. Black contours (25-m intervals) represent the depth of the maximum shears based on the current profiles from the moored ADCP. Cross-track (x) and along-track (y) are normalized by the Rmax of 32 km.

Observed current shear profiles were estimated over 4-m vertical scales for each time sample following hurricane passage at arrays 8 and 9 are shown in Figure 4. Notice that the shear magnitudes are typically two to three times larger than observed in the Loop Current during Lili's passage. This is not surprising since these measurements were acquired in the Gulf Common Water (Nowlin and Hubertz, 1972) and similar to those documented during hurricane Gilbert's passage where up to 3.5^{o}C cooling was observed. In the near-inertial wave wake (Shay *et al*., 1998), the key issue is how much of the current shear is associated with near-inertial wave processes. Compared to the Gulf Common Water, the presence warm and cold eddies significantly impact these levels of near-inertial wave (and shear) activity (Jaimes and Shay, 2010). This is now being explored prior to comparing these values to those from the HYCOM model for each of the experiments discussed above.

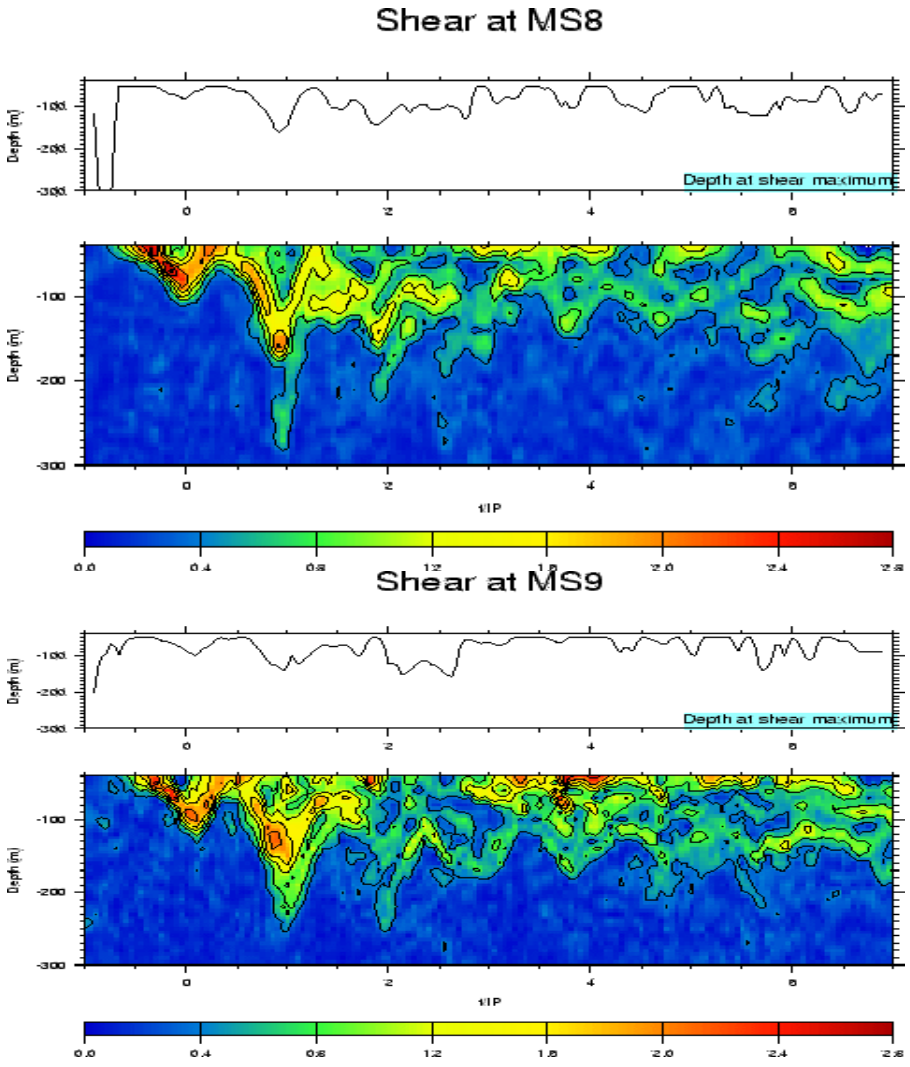

Figure 4: Time series (normalized by inertial period) of observed current shear magnitudes (colored contours) and the respective depths (m) of maximum current shears observed at Moorings 8 (upper: along Ivan' s track) and 9 (lower: 1.5 R_{max} to the right of the Ivan) relative to the time of the closest approach. Shears are normalized by a value of 1.5 x 10^{-2} s^{-1} that have been observed in the Loop Current (Shay and Uhlhorn, 2008).

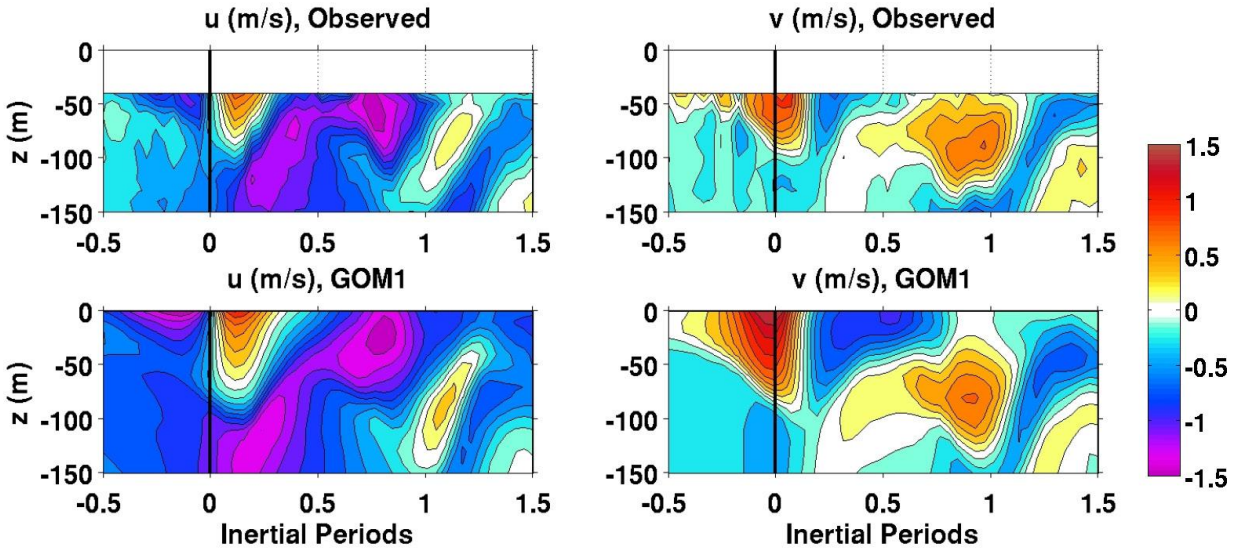

Figure 5: Time series (normalized by inertial period) of observed current components (top panels) and simulated current components from the control Ivan experiment GOM1 in m s^{-1} at SEED Mooring 9.

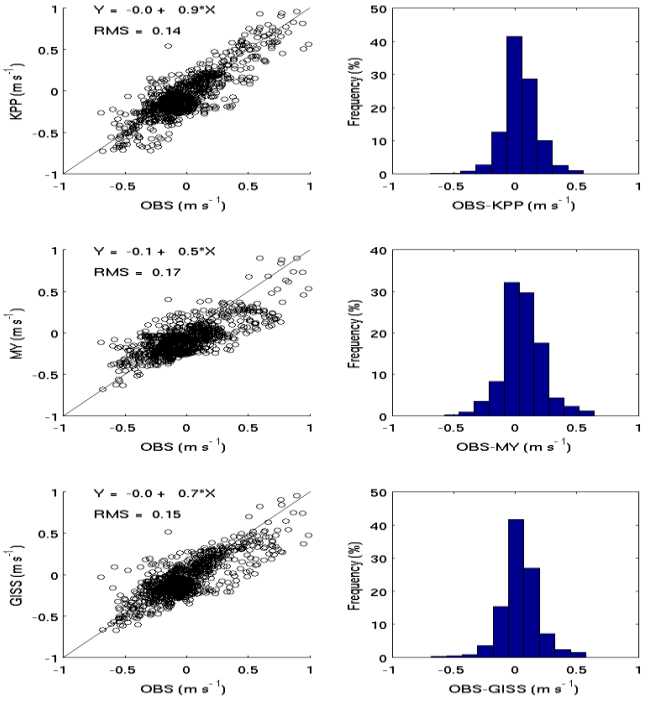

Figure 6: Scatter plot of observed (abscissa) and simulated (ordinate) v-component of the current (left panels) and the histograms of the observed and simulated differences (right panels) in m s^{-1} using KPP, MY and GISS mixing models. Scatter plots have the equation of the regression line as well as the RMS differences between them.

Model versus Observed Current Comparisons: At mooring 9 (Figure 5), velocity component profiles from the control experiment GOM1 are compared to the observed profiles over the upper 150 m. Good agreement exists between observed and simulated currents over the first two inertial periods. These observations and simulations suggest vertical energy propagation out of the surface mixed layer and into the thermocline consistent with theory. Velocity comparisons reveal differences among the three vertical mixing schemes evaluated in GOM1, GOM5, and GOM6. Given the same initialization, wind forcing and drag coefficient formulation as well as

the same number of layers, the KPP scheme used in GOM1 duplicates the observed profiles better than the other two schemes. As shown in Figure 6, the simulations and observations are regressed and fit to a line in a least squares sense. For the comparison with KPP mixing model, the slope between observed and simulated cross-track current is 0.9 with no bias, suggestive of good correlation with RMS difference of 0.14 m s^{-1}. This is reflected in the histogram of the differences. By contrast, the MY (GOM5) and GISS (GOM6) comparisons suggest larger RMS differences and slopes of 0.5 and 0.7, respectively. The distribution of the differences reflects the lower correlation and the increased scatter. Thus these results point to the KPP scheme being superior to both the MY and GISS schemes, at least for this storm at this location. We are now working on comparing the simulations to observed currents and shears from the other 13 ADCPs.

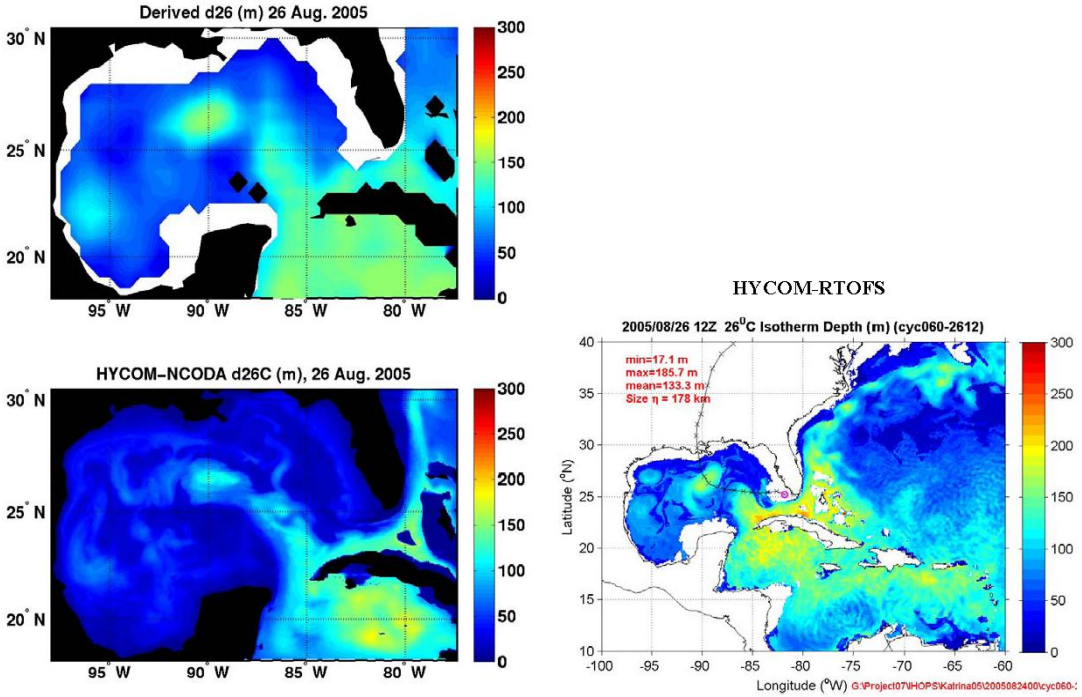

Figure 7. Maps of the depth of the 26°C isotherm derived from satellite altimetry and SST (upper left), obtained from the HYCOM-NCODA ocean hindcast produced by NRL (lower left), and obtained from the HYCOM-RTOFS ocean hindcast produced by NOAA/NCEP/EMC

Interactions with NOAA/NCEP/EMC: A major goal of this project is to interact with the HWRF developers at EMC to evaluate the performance of HYCOM in the next-generation HWRF model and to improve the performance of the ocean model. As part of this effort, G. Halliwell visited EMC during June 2008, presented a seminar highlighting results of the hurricane Ivan evaluation, and interacted with model developers to optimize the ocean model code for the planned 2008 tests of the next-generation HWRF. Evaluation of these tests are now commencing for an HWRF forecast of hurricane Katrina. The first significant result involves evaluating the pre-Katrina initialization of the ocean model. The EMC tests initialize the model with ocean fields produced by their in-house Atlantic Ocean hindcasts using the Real-Time Ocean Forecast System (RTOFS). Comparisons of the depth of the 26°C isotherm between values derived from satellite altimetry and the RTOFS analysis demonstrate that the RTOFS realistically reproduces the magnitude and pattern of this field (Figure 7). The RTOFS field is more realistic than the field produced by the NRL-NCODA data-assimilative hindcast, even

though both assimilation systems use HYCOM. This is encouraging given the paramount importance of proper ocean model initialization (Figure 1). Although the RTOFS initialization for Katrina is realistic, additional storms must be considered to produce a thorough evaluation of this product for ocean model initialization.

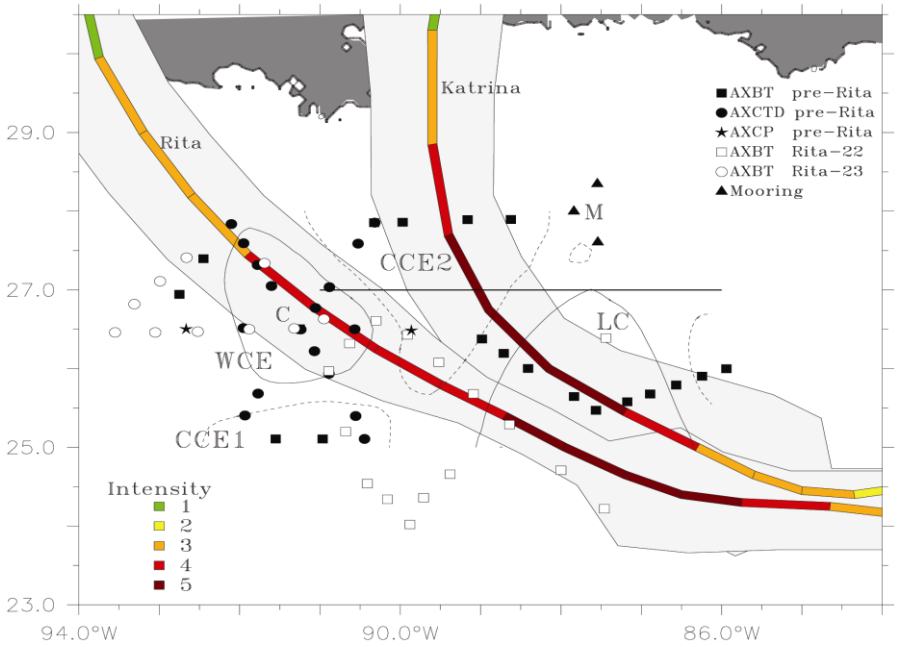

Figure. 8: Airborne profilers deployed in Sept 2005 relative the track and intensity of hurricanes Katrina and Rita (colored lines, with color indicating intensity as per the legend) over the LC System. The light-gray shades on the sides of the storm tracks represent twice the radius of maximum winds (R_{max}). The contours are envelops of anticyclonic (solid: WCE and LC) and cyclonic (dashed: CCE1 and CCE2) circulations. A set of AXBTs (not shown) was deployed after hurricane Rita (26 Sept), following a sampling pattern similar to pre-Rita (or post Katrina) (15 September). Point M indicates the position of several MMS moorings used during this study, and Point C represents the drop site for profiler comparison (AXBT versus AXCTD). The transect along 27^{o}N indicates the extent of vertical sections discussed in the text.

Katrina and Rita: The 3-D upper ocean thermal and salinity structure in the LC system was surveyed with Airborne eXpendable BathyThermographs (AXBT), Current Profilers (AXCP), and Conductivity-Temperature-Depth sensors (AXCTD) deployed from four aircraft flights during September 2005, as part of a joint NOAA and National Science Foundation experiment (Rogers *et al.*, 2006; Shay, 2009). Flight patterns were designed to sample the mesoscale features in the LC system: the LC bulge (amplifying WCE), the WCE that separated from the LC about two days before the passage of Rita, and two CCEs that moved along the LC periphery during the WCR shedding event (Fig. 8). The first aircraft flight was conducted on 15 Sept (two weeks after Katrina or one week before Rita, i.e. pre-Rita), the second and third flights were conducted during Rita's passage (22 and 23 Sept, respectively), and the final flight was conducted on 26 Sept, a few days after Rita's passage. Pre-Rita and post-Rita (not shown) flights followed the same pattern, while these other Rita flights focused on different regions along Rita's track. Data acquired during pre-Rita includes temperature profilers from AXBTs, temperature and salinity profilers from AXCTDs, and current and temperature profilers from two AXCPs deployed in the western and eastern sides of the WCE (Jaimes and Shay 2009). A salient characteristic of the

WCE is the salinity maximum of ~36.4 to 36.7 practical salinity units. This behavior must be incorporated into numerical models, as a climatological salinity profile is insufficient to accurately initialize an model ocean with a WCE. Realistic salinity profiles to match the temperature profiles would then resolve horizontal density gradients and the corresponding geostrophic flows associated with oceanic features (Shay *et al.*, 1998).

The combination of these airborne profiles of temperature and salinity measurements with the MMS-sponsored ADCP and CTD moorings were fairly consistent. These continuous measurements of ocean temperatures, salinities (via conductivities), and currents were acquired from the mooring sensors at intervals of 0.5 and 1 hr for CTDs and ADCPs, respectively. Although the moorings were located outside the radius of maximum winds R_{max} of hurricanes Katrina (~4.5 R_{max} where R_{max} = 47 km) and Rita (~17.5 R_{max} where R_{max} = 19 km) (Fig. 8), CCE2 that was affected by Katrina (category 5 status) propagated over the mooring site ≈2 days after interacting with the storm. The circulation of the LC bulge that interacted with Rita (category 5 status) extended over the mooring ≈3 days after having been affected by the storm. The cluster averages of the thermal structure revealed that the LC cooled by 1°C, the WCE temperature cooled by 0.5°C, and the eddy shedding region and the CCE cooled by more than 4.5°C (Jaimes and Shay 2009). These profiles will represent a challenge for the model especially placing the oceanic features in the correct position as suggested by the Ivan model analyses (Halliwell *et al.*, 2009).

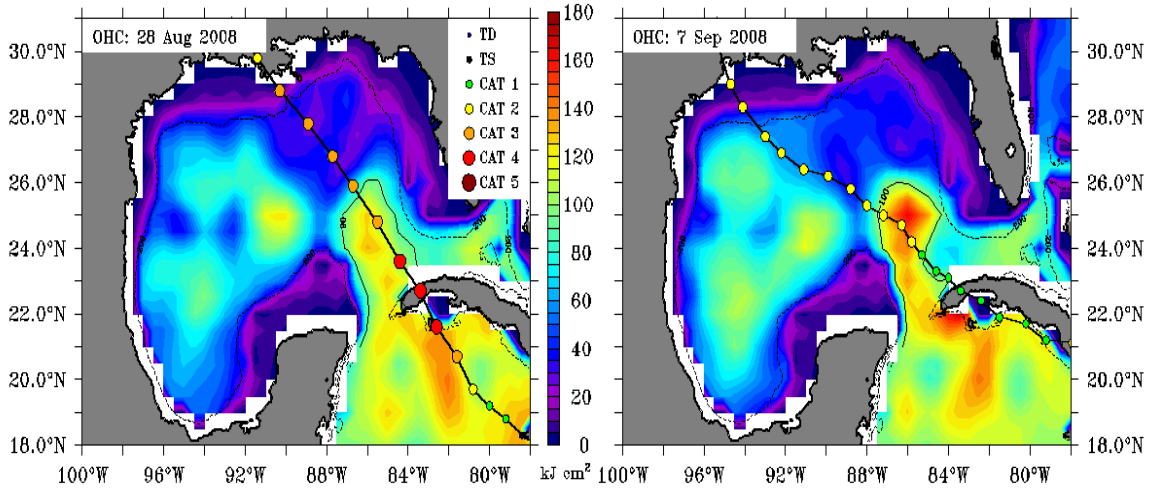

Figure 9: Track (black line) and intensity (circles:legend) of hurricanes a) Gustav and b) Ike relative to the pre-storm OHC (kJ cm^{-2}) distributions in the Gulf of Mexico prior to their passages on 28 Aug and 7 Sep 2008.

Gustav and Ike: More recently, hurricane Gustav and Ike moved over the Gulf of Mexico and interacted with the LC and the eddy field in August and September 2008 (Fig. 9). As part of the NCEP tail Doppler Radar Missions, oceanic and atmospheric measurements were acquired on sixteen NOAA WP-3D research flights for pre, during and post-storm flights. In total, over 400 AXBTs and 200 GPS sondes were deployed to document the evolving atmospheric and oceanic structure over warm and cooler ocean features in these two hurricanes (Table 4). In addition, forty-five GPS sondes were deployed on 1 Sept over the float and drifter array deployed by the United States Air Force WC-130J north and west of the Loop Current. Similar to CBLAST

observations, the float array also included the EM/APEX floats that measure the horizontal velocities as well as temperature and salinity structure (Sanford *et al*., 2007). However, this effort significantly improved upon the CBLAST effort in that the forcing is better documented with the combination of GPS sondes and the Stepped Frequency Microwave Radiometer (Uhlhorn *et al.*, 2007) directly over the float and drifter array. In addition, each research flight carried AXBTs to document the evolving upper ocean thermal structure across the entire Gulf of Mexico for the first time. Note that the AXBTs were deployed to document pre- and post-storm oceanic variability in the Loop Current and its periphery where float and drifter measurements would be advected away from the storm track by the energetic ocean current. This is precisely why we need current profilers to deploy from the research aircraft on a routine basis.

Table 4: Summary of atmospheric (GPS) and oceanic (AXBT) profiler measurements from sixteen flights acquired in hurricanes Gustav and Ike in 2008. Numbers in parentheses represent profiler failures.

Hurricane Gustav				Hurricane Ike			
Date	Flight	GPS	AXBT	Date	Flight	GPS	AXBT
(2008)				(2008)			
28 Aug	RF43	0	49(2)	08 Sep	RF43	0	47(2)
29 Aug	RF42	12(4)	16(0)	09 Sep	RF42	19	6(0)
30 Aug	RF43	9	19(2)	10 Sep	RF42	17(1)	10(2)
31 Aug	RF42	24	16(1)	10 Sep	RF43	11	20(7)
31 Aug	RF43	17(2)	19(1)	11 Sep	RF42	16	10(1)
01 Sep	RF43	44	19	11 Sep	RF43	10	22(3)
03 Sep	RF43	4	54(4)	12 Sep	RF42	21(2)	10(4)
				12 Sep	RF43	8	20(4)
				15 Sep	RF43	0	61(5)
Total	7	111(6)	191(10)		9	111(3)	216(28)

Summary: We made significant progress on this grant as the numerical simulations with ocean conditions observed during hurricane Ivan's passage by Walker *et al*. (2005). Warm and cold eddies suggest regimes of less and more negative feedback to the atmosphere. We have completed the analysis of Ivan within the context of mixing and upwelling and downwelling processes by comparing simulations of the currents and shears to *in situ* measurements from the SEED moorings (Teague *et al*., 2007). In addition, we have started the pre- Katrina and Rita cases will be evaluated with model simulations and observations, as well as Gustav and Ike pre-storm states. These combined numerical and observational efforts here have benefitted from a PhD student (Jaimes 2009) to examine model sensitivities and comparing these simulations to the NRL and MMS profiler measurements. Given the 5-year program of the recently funded Dynamics of the Loop Current Study, this project will benefit from in-situ mooring data as well as the detailed aircraft measurements that will be acquired during the NOAA IFEX, NASA GRIP, and NSF PREDICT experiments during the summer of 2010. Our focus will be on the

Gulf of Mexico's Loop Current region where hurricanes can rapidly weaken or deepen as they interact with warm and cold ocean features.

Acknowledgments: This study has benefited from the interactions with Mr. William Teague in the Oceanography Department at the US Naval Research Laboratory at Stennis Space Center, Dr. Alexis Lugo-Fernandez at Minerals Management Service sponsored ADCP moorings. This project has also benefited from continuing support from the National Science Foundation (Dr. Stephen Nelson) in the acquisition and analysis of measurements acquired during hurricanes in collaboration with NOAA's Hurricane Research Division (Drs. Frank Marks, Rob Rogers, Eric Uhlhorn) and Aircraft Operations Center (Dr. James McFadden). Dr. Benjamin Jaimes also contributed to this effort.

References and Publications(*):

Donelan, M. A., B. K. Haus, N. Reul, W. J. Plant, M. Stiassine, H. Graber, O. Brown, and E. Saltzman, 2004: On the limiting aerodynamic roughness of the ocean in very strong winds. Geophys. Res. Letters., 31L18306,doi:1029/2004GRL019460.

*Halliwell, G., L. K. Shay, S. D. Jacob, O. Smedstad, and E. Uhlhorn, 2008: Improving ocean model initialization for coupled tropical cyclone forecast models using GODAE nowcasts. Mon. Wea Rev., 136 (7), 2576–2591.

*Halliwell, G. R., L. K. Shay, J. Brewster, and W. J. Teague. 2010: Evaluation and sensitivity analysis to an ocean model response to hurricane Ivan. Mon. Wea. Rev. **(Accepted subject to revision)**

*Jaimes, B., 2009: On the oceanic response to tropical cyclones in mesoscale ocean eddies. PhD Dissertation. Division of Meteorology and Physical Oceanography, Rosenstiel School of Marine and Atmospheric Science, University of Miami, Miami, FL 33149, 143 pp.

*Jaimes, B. and L. K. Shay. 2009: Mixed layer cooling in mesoscale eddies during Katrina and Rita. Mon. Wea. Rev., 20 pp., doi: 10.1175_2009MWR.pdf **(In Press)**

*Jaimes, B. and L. K. Shay, 2010: Near-inertial wave wake of hurricanes Katrina and Rita in mesoscale eddies. J. Phys. Oceanogr.. **(Accepted subject to revision)**

Jarosz, E., D. A. Mitchell, D. W. Wang, and W. J. Teague, 2007: Bottom-up determination of air-sea momentum exchange under a major tropical cyclone. Science, 315, 1707-1709.

*Mainelli, M., M. DeMaria, L. K. Shay and G. Goni. 2008: Application of oceanic heat content estimation to operational forecasting of recent category 5 hurricanes, Wea and Forecast., 23(1), 3-16.

Murphy, A. H., 1988. Skill scores based on the mean square error and their relationships to the correlation coefficient. *Mon. Wea. Rev.*, **116**, 2417-2424.

Nowlin, W. D. Jr., and J. M. Hubertz, 1972: Contrasting summer circulation patterns for the eastern Gulf. In: Contributions on the Physical Oceanography of the Gulf of Mexico, Tex. A&M Oceanogr. Stud., vol. 2, edited by L. R. A. Capurro and J. L. Reid, pp. 119-138, Gulf Pub. Co.

Reynolds, R. W., T. M. Smith, C. Liu, D. B. Chelton, K. S. Casey, and M. G. Schlax, 2007: Daily high-resolution blended analyses for sea surface temperature. *J. Climate*, **20**, 5473-5496.

Rogers, R., S. Aberson, M. Black, P. Black, J. Cione, P. Dodge, J. Dunion, J. Gamache, J. Kaplan, M. Powell, L. K.Shay, N. Surgi, E. Uhlhorn, 2006: The intensity forecasting experiment (IFEX), a NOAA multiple year field program for improving intensity forecasts. BAMS, 87(11), 1523-1537.

*Rappaport, E. N., J. L. Franklin, M. DeMaria, A. B. Shumacher, L. K. Shay and E. J. Gibney, 2010: Tropical cyclone intensity change before U. S. Gulf coast landfall. Wea. and Forecast., **(Submitted)**

Sanford, T B., J. F. Price, J. Girton, and D. C. Webb, 2007: Highly resolved observations and simulations of the oceanic response to a hurricane. Geophys. Res. Lett., 34, L13604, 5 pp.

*Shay, L.K., 2009: Upper Ocean Structure: a Revisit of the Response to Strong Forcing Events. In: Encyclopedia of Ocean Sciences, ed. John Steele, S.A. Thorpe, Karl Turekian and R. A. Weller, Elsevier Press International, Oxford, UK, 4619-4637, doi: 10.1016/B978-012374473-9.00628-7.

*Shay, L. K.,2010: Air-Sea Interactions in Tropical Cyclones (Chapter 4). In Global Perspectives of Tropical Cyclones, 2nd Edition, Eds. Johnny C. L. Chan and C. P. Chang, World Scientific Publishing Company: Earth System Science Publication Series, London, UK, 45 pp **(In Press)**.

Shay, L. K., A. J. Mariano, S. D. Jacob, and E. H. Ryan, 1998: Mean and near-inertial response to hurricane Gilbert. J. Phys. Oceanogr., 28, 858–889.

*Shay, L. K. and E. Uhlhorn, 2008: Loop Current Response to hurricanes Isidore and Lili, Mon. Wea. Rev., 137, 3248-3274.

*Shay, L. K., and J. Brewster, 2009: Oceanic heat content variability in the eastern Pacific Ocean for hurricane intensity forecasting. Mon. Wea. Rev., **(Accepted subject to revision)**.

Taylor, K. E., 2001: Summarizing multiple aspects of model performance in a single diagram. *J. Geophys. Re*s., **106**, 7183-7192.

Teague, W. J., E. Jarosz, D. W. Wang, and D. A. Mitchell, 2007: Observed oceanic response over the upper continental slope and outer shelf during Hurricane Ivan, J. Phys. Oceanogr. 37, 2181-2206.

Uhlhorn, E. W., P. G. Black, J. L. Franklin, M. Goodberlet, J. Carswell and A. S. Goldstein, 2007:Hurricane surface wind measurements from an operational stepped frequency microwave radiometer. Mon. Wea. Rev., 135, 3070-3085.

*Uhlhorn, E. W., 2008: Gulf of Mexico Loop Current mechanical energy and vorticity response to a tropical cyclone. PhD Dissertation. RSMAS, University of Miami, Miami, FL 33149, 148 pp.

Walker, N., R. R. Leben, and S. Balasubramanian 2005: Hurricane forced upwelling and chlorophyll a enhancement within cold core cyclones in the Gulf of Mexico. Geophys. Res. Letter, 32, L18610, doi: 10.1029/2005GL023716, 1-5.